Chemical Form Matters: Differential Accumulation of Mercury Following Inorganic and Organic Mercury Exposures in Zebrafish Larvae

Malgorzata Korbas,[†,¶] Tracy C. MacDonald,[†,‡,¶] Ingrid J. Pickering,[†] Graham N. George,[†,‡,§,*] and Patrick H. Krone[‡,§]

[†]Molecular and Environmental Science Research Group, Department of Geological Sciences, University of Saskatchewan, Saskatoon, SK, S7N 5E2, Canada

[‡]Toxicology Centre, University of Saskatchewan, Saskatoon, SK, S7N 5B3, Canada

[§]Department of Anatomy and Cell Biology, University of Saskatchewan, Saskatoon, SK, S7N 5E5, Canada

Ⓢ *Supporting Information*

ABSTRACT: Mercury, one of the most toxic elements, exists in various chemical forms each with different toxicities and health implications. Some methylated mercury forms, one of which exists in fish and other seafood products, pose a potential threat, especially during embryonic and early postnatal development. Despite global concerns, little is known about the mechanisms underlying transport and toxicity of different mercury species. To investigate the impact of different mercury chemical forms on vertebrate development, we have successfully combined the zebrafish, a well-established developmental biology model system, with synchrotron-based X-ray fluorescence imaging. Our work

revealed substantial differences in tissue-specific accumulation patterns of mercury in zebrafish larvae exposed to four different mercury formulations in water. Methylmercury species not only resulted in overall higher mercury burdens but also targeted different cells and tissues than their inorganic counterparts, thus revealing a significant role of speciation in cellular and molecular targeting and mercury sequestration. For methylmercury species, the highest mercury concentrations were in the eye lens epithelial cells, independent of the formulation ligand (chloride *versus* L-cysteine). For inorganic mercury species, in absence of L-cysteine, the olfactory epithelium and kidney accumulated the greatest amounts of mercury. However, with L-cysteine present in the treatment solution, mercuric bis-L-cysteineate species dominated the treatment, significantly decreasing uptake. Our results clearly demonstrate that the common differentiation between organic and inorganic mercury is not sufficient to determine the toxicity of various mercury species.
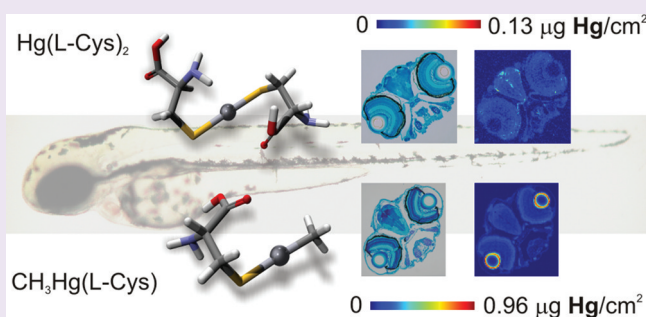
Compounds of heavy elements are often toxic, and excluding radioactive elements, compounds of mercury are generally the most toxic. In natural systems mercury is found in elemental, inorganic, and organometallic forms. The nature and extent of mercury toxicity depend largely on its molecular form.[1] Relatively benign mercury compounds include mercuric sulfides which have very low solubilities; α-HgS is widely used in traditional Chinese medicines[2] and in red tattoo ink,[3] while β-HgS occurs on the surface of aged dental amalgam restoratives.[4] In contrast, organo-mercury compounds are extremely toxic to vertebrates, for example dimethylmercury is one of only a few compounds formally classified as supertoxic.[5]

Human populations are exposed to different forms of mercury from a wide variety of sources. Exposure to elemental and inorganic mercury comes mainly from dental amalgams and inhalation of ambient air during occupational activities (chlor-alkali plants, mercury mines, mercury-based gold and silver mining), as well as from direct contact with mercury-containing products (*e.g.*, thermometers and other measuring equipment, batteries, fluorescent light bulbs) and ingestion of mercury-contaminated food and water.[6] Exposure to elemental and inorganic mercury is especially high in Asia, the region with both the largest mercury emissions[7] and the highest demand for this metal.[8] In some Asian countries the continuous use of traditional, folk or herbal medicines containing metallic or inorganic mercury also contributes to elevated exposures.[9]

The dominant organic mercury form to which humans are exposed is thiolate-bound methylmercury.[10] This compound is present in virtually all fish and seafood products and exposure is therefore more widespread than to other forms of mercury. Concentrations of mercury in fish vary between species and

habitats, with generally higher levels in carnivorous and older fish or fish from polluted areas. The levels of human exposure to methylmercury strongly depend on fish and seafood eating habits and may be elevated among populations reliant on these foodstuffs for their daily nutrition.[11−13]

The adverse effects of mercury on health depend on chemical form and dose; however, mercury vapor and organic mercury have one common characteristic. They readily cross the blood-brain (BBB) and blood-placental barrier (BPB) causing irreversible damage to the nervous system especially in early stages of development.[1] In contrast, inorganic mercury (e.g., mercuric mercury, Hg^{2+}) has limited capacity to cross the BBB and BPB but is avidly accumulated by the kidneys.[1] Although mercuric mercury is generally less toxic than organic forms, it plays a key role in mercury toxicology. The mercuric ion is produced in tissues after inhalation of mercury vapor. It is also a product of methylmercury demethylation in the intestines and the brain.[14] The WHO have estimated that the average daily mercury intake in North America and Europe is approximately 4.3 and 2.4 μg for inorganic and organometallic forms, respectively, with most of the latter arising from fish.[15] Even though these levels are not high, mercury accumulation within the human body over time may be a problem. A recent study confirmed that inorganic mercury deposition within the body due to chronic exposure increases with age and correlates significantly with biological markers of the main mercury targets: pituitary, immune system, and liver.[16]

Early life stages are particularly susceptible to mercury's adverse effects; however, the mechanisms of mercury disposition within the developing body are poorly understood. Zebrafish makes an excellent model vertebrate to study mercury toxicity in developing organisms,[17] especially due to an endothelial-based BBB, which exhibits characteristics comparable to its mammalian counterpart as early as 3 days post fertilization (dpf).[18] Previously we successfully utilized zebrafish with synchrotron-based X-ray fluorescence imaging to study the localization, dynamic accumulation, and redistribution of mercury in developing zebrafish embryos and larvae following waterborne exposure to methylmercury L-cysteineate.[19,20] Here we investigate the uptake of different organic and inorganic mercury species in zebrafish larvae, showing that mercury accumulation patterns vary tremendously with the chemical form.

RESULTS AND DISCUSSION

Solution Species and the Nature of the Exposure.
Zebrafish larvae at 3.5 dpf were exposed for 36 h to four different mercury formulations in water: 1 μM mercuric chloride, 1 μM methylmercury chloride, 200 μM mercuric bis-L-cysteineate, and 2 μM methylmercury L-cysteineate. The mercury treatment concentrations were chosen to be non-lethal over the exposure period and to facilitate detection in larval tissues. Preliminary range-finding experiments demonstrated considerable differences in toxicity with chemical forms, especially for the L-cysteine based forms, thus precluding the use of identical concentrations for all mercury forms. In particular, mercuric bis-L-cysteineate showed very low toxicity to developing larvae; even at 200 μM it did not cause any deformities or behavioral changes, although low death rates were observed with longer exposures in some experiments (96 h).

The complex water chemistry potentially present in the exposure solutions was estimated using the simulation program MINTEQA2.[21] Consistent with previous work, solution mercury speciation was predicted to depend on pH and the concentrations of chloride and L-cysteine.[22−24]

Due to low chloride content in the zebrafish culture water (~0.31 mM) and the slightly basic pH (7.8), the predominant inorganic and organic mercury forms (in absence of L-cysteine) were predicted to be uncharged hydroxide complexes, Hg-$(OH)_2$ and CH_3HgOH (Table 1). The total concentration of

Table 1. Predicted Mercury Speciation in Zebrafish Culture Water[a]

formulation[b]	mercury species	mol %
1 μM $HgCl_2$	$Hg(OH)_2$	90.0
	HgClOH	9.5
	$HgCO_3$	0.3
	$HgCl_2$	0.2
1 μM CH_3HgCl	CH_3HgOH	96.1
	CH_3HgCl	3.3
	CH_3HgCO_3	0.6
200 μM $HgCl_2$ + 500 μM L-Cys	$Hg(L-Cys)_2$	100.0
2 μM CH_3HgOH + 2.4 μM L-Cys	$CH_3Hg(L-Cys)$	100.0

[a]Computed at 28 °C and pH 7.8 using MINTEQA2. [b]Other components originating from system water, phosphate buffered saline (PBS) formulation, and HEPES buffer are given in Supplementary Table 1.

$Hg(OH)_2$ was well below its water solubility of 0.25 mM;[25] consistent with this no precipitation was observed. Figure 1
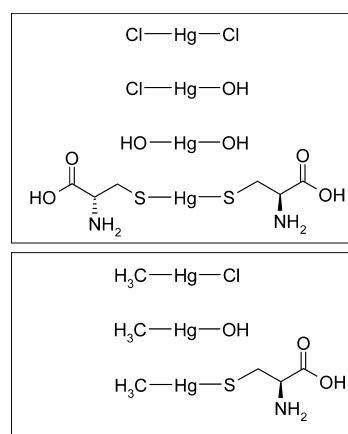

Figure 1. Schematic structures of the inorganic and organic mercury species considered in this work.

shows structures of the different mercury species considered. These species are in equilibrium, with differing uptake rates of the specific equilibrating species; removal of one species from solution by uptake will drive the equilibrium to replenish that species. To study the effects of individual equilibrating components would require variation of conditions such as chloride and pH, which would affect the larvae in complex ways; this is outside the present scope. For the L-cysteine complexes, essentially all of the mercury was predicted to be thiol-bound (Table 1) as expected from the high affinities of mercury for thiolates.[26] This is illustrated by the formation constant for methylmercury L-cysteineate of $10^{15.7}$, compared with $10^{5.45}$ and $10^{9.5}$ for chloride and hydroxide forms, respectively.[26]
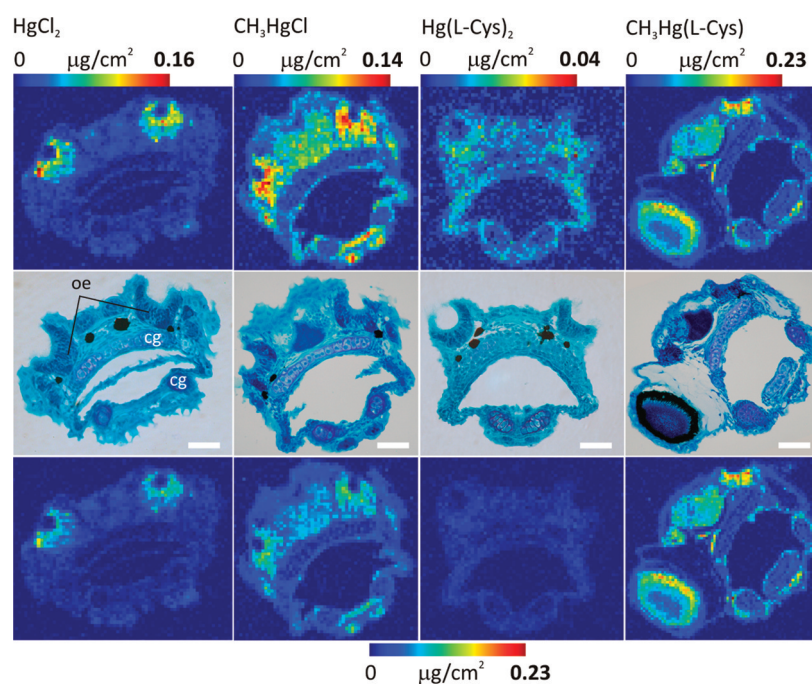
Figure 2. Quantitative mercury distributions in 5 dpf zebrafish larvae following a 36-h exposure to 1 μM mercuric chloride HgCl$_2$, 1 μM methylmercury chloride CH$_3$HgCl, 200 μM mercuric bis-L-cysteineate Hg(L-Cys)$_2$, or 2 μM methylmercury L-cysteineate. The dominant mercury species in the treatment solutions are shown in Table 1. Histological images (middle panel) of olfactory epithelium are compared with the mercury distributions of the adjacent sections. The first row mercury maps are scaled separately to the highest level of mercury in each of the images, whereas the ones in the third row are scaled to the highest level of mercury among all four images. Scale bar 50 μm; oe, olfactory epithelium; cg, cartilage.
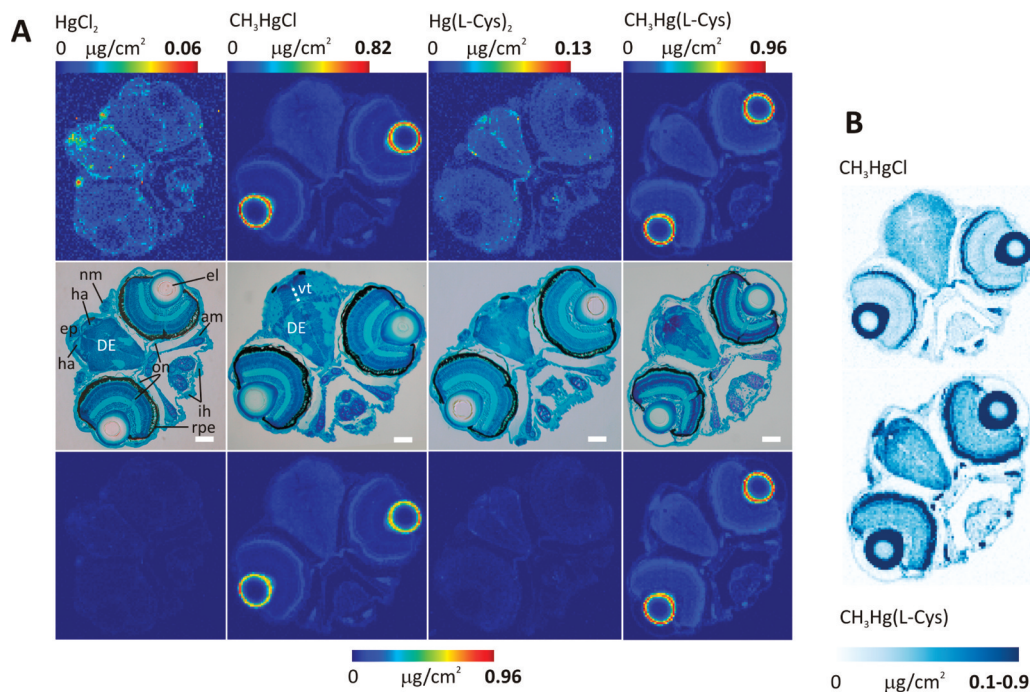

Figure 3. Quantitative mercury distributions in 5 dpf zebrafish larvae following a 36-h exposure to 1 μM mercuric chloride HgCl$_2$, 1 μM methylmercury chloride CH$_3$HgCl, 200 μM mercuric bis-L-cysteineate Hg(L-Cys)$_2$, or 2 μM methylmercury L-cysteineate. The dominant mercury species in the treatment solutions are shown in Table 1. Histological images (middle panel) of the brain and the eye are compared with the mercury distributions of the adjacent sections (A). The first row mercury maps are scaled separately to the highest level of mercury in each of the images, whereas the ones in the third row are scaled to the highest level of mercury among all four images. Scale bar 50 μm; el, eye lens, rpe, retinal pigmented epithelium; on, optic nerve; nm, neuromast; ih, interhyoideus; am, adductor mandibulae; ep, epiphysis; ha, habenula; vt, ventricular region; DE, diencephalon. Mercury distribution maps for organic mercury exposures were scaled to 0.1 μg/cm^2 to better illustrate the variations in the mercury levels in the brain region (B).
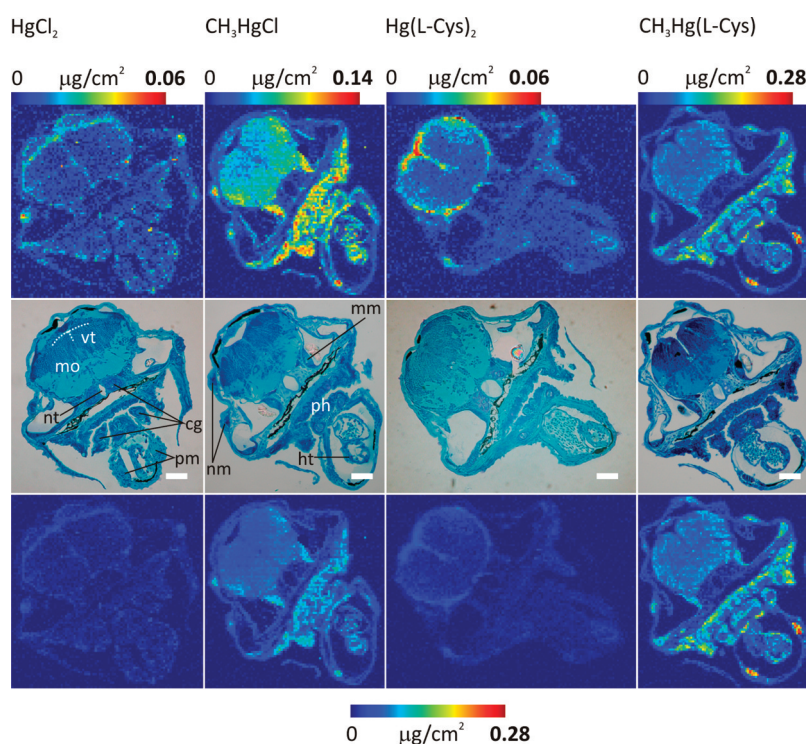
Figure 4. Quantitative mercury distributions in 5 dpf zebrafish larvae following a 36-h exposure to 1 μM mercuric chloride $HgCl_2$, 1 μM methylmercury chloride CH_3HgCl, 200 μM mercuric bis-L-cysteineate $Hg(L$-$Cys)_2$, or 2 μM methylmercury L-cysteineate. The dominant mercury species in the treatment solutions are shown in Table 1. Histological images (middle panel) of the heart region are compared with the mercury distributions of the adjacent sections. The first row mercury maps are scaled separately to the highest level of mercury in each of the images, whereas the ones in the third row are scaled to the highest level of mercury among all four images. Scale bar 50 μm; vt, ventricular region; mo, medulla oblongata; nt, notochord; pm, pericardial muscles; cg, cartilage; nm, neuromast; mm, median macula; ph, pharynx; ht, heart.

Tissue and Chemically Specific Mercury Accumulation.

For each exposure condition, four transverse sections representing different tissues and organs were imaged and analyzed for mercury distribution. In all cases, untreated control fish showed no mercury signal. The use of the high flux 5-μm-size synchrotron X-ray beam from 20-ID-B at the Advanced Photon Source significantly improved mercury detection at lower concentrations and with higher spatial resolution than our previous work.[19,20]

Figure 2 compares 5-μm-resolution X-ray fluorescence images showing mercury distributions in 6-μm-thick olfactory epithelium sections of exposed zebrafish larvae. The mercury distribution substantially varied with the exposure chemical form. Despite the extremely high concentration for the mercuric bis-L-cysteineate exposure (200 μM), mercury levels in treated larvae were extremely low (less than 0.04 μg/cm^2) with no specific tissue targeted (Figure 2). In contrast, uptake in mercuric chloride-treated larvae was highly efficient and selective with highly elevated mercury only in olfactory epithelium (up to four times that from mercuric bis-L-cysteineate exposure). The olfactory epithelium contains the sensory hair cells required for olfaction. Organic mercury uptake in the olfactory section was more widespread than for mercuric chloride. In both methylmercury chloride solution- and methylmercury L-cysteineate-treated larvae, significant mercury accumulated not only in the olfactory epithelium (up to 0.14 and 0.21 μg/cm^2, respectively) but also in other tissues (Figure 2). Despite these differences, all four mercury forms showed very low mercury uptake by cartilage cells accompanied by higher mercury uptake by surrounding connective tissue (Figure 2), possibly due to the relatively low cell density and avascularity of cartilage.

Given the known toxic effects of mercury on the brain, mercury distributions in transverse sections through the brain and eye were next examined (Figure 3). Figure 3A shows striking differences in mercury uptake between inorganic and organic species. Overall mercury levels were significantly lower for inorganic compared to organic mercury species. Following exposure to mercuric chloride solutions (Figure 3A), mercury specifically concentrated in the neuromasts, epiphysis (pineal gland), and brain ventricular region. Trace mercury was detected in other tissues including the optic nerve. With mercuric bis-L-cysteineate exposure, the brain area appeared preferentially targeted; tissues with the highest mercury levels included the epiphysis, ventricular region, habenula, and optic nerve (Figure 3A).

The mercury accumulation patterns following exposures to organic mercury were very distinct from those from the inorganic species and virtually independent of the bound ligand (Figure 3). For both methylmercury chloride and methylmercury L-cysteineate solutions, the highest mercury levels were detected in the outer layer of the eye lens (Figure 3A; up to 0.82 and 0.96 μg/cm^2, respectively), corresponding to the lens epithelium, a single layer of dividing cells that gives rise to fibers within the lens; these data confirm these cells as a major target organ for organic mercury.[19,20] Levels in lens epithelium were on average 3−5 times higher than in the outermost layers of the retina (most likely retinal pigmented epithelium and/or photoreceptor layer), the second highest mercury uptake site within the eye section. Similar mercury levels to those found in the retina were also observed in the cranial muscles, namely,
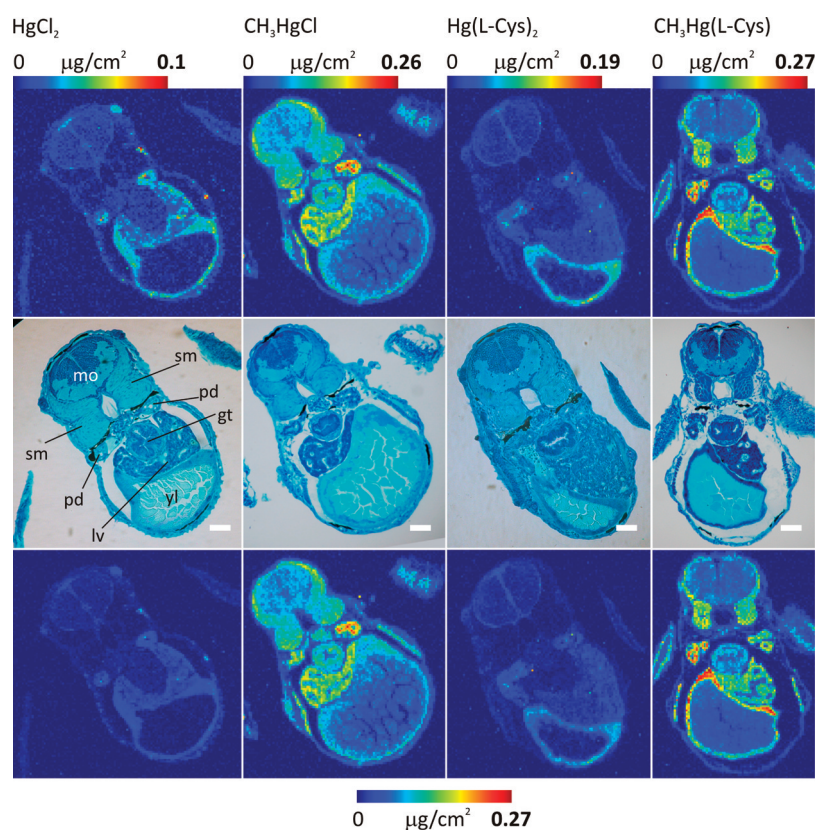
Figure 5. Quantitative mercury distributions in 5 dpf zebrafish larvae following a 36-h exposure to 1 μM mercuric chloride HgCl$_2$, 1 μM methylmercury chloride CH$_3$HgCl, 200 μM mercuric bis-L-cysteineate Hg(L-Cys)$_2$, or 2 μM methylmercury L-cysteineate. The dominant mercury species in the treatment solutions are shown in Table 1. Histological images (middle panel) of the liver region are compared with the mercury distributions of the adjacent sections. The first row mercury maps are scaled separately to the highest level of mercury in each of the images, whereas the ones in the third row are scaled to the highest level of mercury among all four images. Scale bar 50 μm; mo, medulla oblongata; sm, somitic muscles; pd, pronephric duct; gt, gut; lv, liver; yl, yolk.

adductor mandibulae and interhyoideus. However, consistent with the olfactory sections, very low mercury uptake was observed in the cartilage tissue. Significant mercury also accumulated in the optic nerve with maximum mercury levels for chloride or L-cysteine bound methylmercury exposures at 0.085 and 0.19 μg/cm^2, respectively. Interestingly, mercury accumulation in the brain region was more diffuse but showed overall significantly higher mercury levels than for inorganic mercury exposures (Figure 3). Following organic mercury exposures, mercury accumulated in the diencephalon of the forebrain region with progressively higher levels with increasing distance from the ventricle. However, no mercury was present within the ventricular region itself, again in striking contrast to the inorganic mercury exposures. Due to a slight difference in the sectioning planes of the two specimens, specific mercury accumulation in the habenula and epiphysis could be observed only in the methylmercury L-cysteineate-treated larva (Figure 3B). The mercury levels in these two were at least 2-fold higher than those of the gray matter of the diencephalon.

Consistent with findings from the olfactory epithelium and eye sections, transverse sections of the heart region showed mercury levels in the inorganic mercury-treated fish that were significantly lower than those treated with the organic forms (Figure 4). Among the two inorganic forms, mercury uptake from mercuric chloride solution was more efficient as similar levels in larvae were observed for the 200 μM mercuric bis-L-cysteineate solutions compared to the 1 μM mercuric chloride solutions. The ventricular region was a common target for both

inorganic mercury treatments with maximum mercury levels at 0.03 and 0.05 μg/cm^2 for mercuric chloride solution and mercuric bis-L-cysteineate exposures, respectively (Figure 4). For the latter treatment, mercury lined the periphery of the medulla oblongata in the hindbrain region protruding in certain areas toward its interior. Other organs such as the pharynx or heart showed only trace levels (below 0.02 μg/cm^2) of accumulated mercury when exposed to inorganic mercury forms. Following organic mercury exposures, the mercury distribution was again higher and more widespread, with notable differences compared to inorganic mercury (Figure 4). Organic mercury treated larvae showed significant mercury throughout the medulla oblongata region. For methylmercury L-cysteineate the distribution was nearly uniform, with mercury levels between 0.04 and 0.09 μg/cm^2. However, for methylmercury chloride solution, the white matter of the medulla oblongata showed slightly higher mercury levels than the gray matter (0.05–0.1 vs 0.03–0.06 μg/cm^2). Interestingly, overall mercury levels in the medulla oblongata for the two organic mercury forms were similar despite the double molar excess of mercury in the methylmercury L-cysteineate solutions compared to the methylmercury chloride solutions. Similarly, comparable mercury levels (0.07–0.13 μg/cm^2) were detected in the median macula (sensory epithelium) of the inner ear following the two organic mercury exposures.

A significant and noteworthy difference between inorganic and organic mercury-exposed larvae was that the former showed specific mercury accumulation in the ventricular region

Table 2. Estimated Diffusion Coefficients and Membrane Permeabilities for Different Mercury Species[a]

permeant	K_{ow}[b]	molecular volume[c] (Å³)	diffusion coefficient D_m (× 10^{-10} cm²/s)	permeability P (× 10^{-4} cm/s)
Hg(OH)₂	0.05	47.9	3.78	0.47
HgClOH	1.2	55.6	1.82	5.45
CH₃HgOH	0.07	54.9	1.94	0.34
CH₃HgCl	1.7	63.0	0.90	3.8
Hg(L-Cys)₂	3.7	189.4	0.0000054	0.00005
CH₃HgL-Cys	50	124.7	0.0025	0.32

[a]D_m and P values are estimated for the passive transport across the human red blood cell membrane. [b]See ref 29. [c]Calculated by Accelrys Discovery Studio (v3.0.0) from the three-dimensional geometry-optimized energy-minimized density functional theory structures as the total van der Waals volume of all atoms subtracted by the overlap volume of bonded atoms and scaled to 95%.

of the brain, whereas the organic mercury was excluded from this region (Figure 4). In addition, the pharyngeal epithelium, the heart, and the pericardial muscles showed significantly elevated mercury levels only with the organic mercury exposures (Figure 4). Interestingly, none of the mercury exposures gave rise to mercury in the notochord or cartilage tissue. Both are highly hydrated, avascular tissues that provide structural support to the developing larva through the development of hydrostatic pressure.

The presence of neuromasts in the heart sections of the organic mercury-treated larvae (Figure 4) and in the eye section of the inorganic mercury-treated larvae (Figure 3) allowed us to compare mercury accumulation in a second type of sensory organ containing sensory hair cells. Unlike the olfactory epithelium, neuromasts are mechanosensory organs responsible for detecting pressure changes in water. By far the highest mercury levels were detected in the neuromasts from larvae treated with organic mercury (0.11 and 0.16 μg/cm² for methylmercury chloride and methylmercury L-cysteineate solutions, respectively). The neuromast mercury levels with mercuric chloride solutions (0.02−0.06 μg/cm²) were on average half of those of the organic counterparts (Figures 3 and 4). The lowest neuromasts mercury accumulation was detected for the mercuric bis-L-cysteineate solutions (less than 0.02 μg/cm²).

Liver sections showed even more pronounced differences in mercury uptake and accumulation between inorganic and organic mercury exposures (Figure 5). Organs especially highlighting those differences included medulla oblongata, the somitic muscles, the gut, and the yolk. In these tissues the levels of mercury following inorganic mercury exposures were negligibly low or even close to zero.

In the case of the mercuric chloride solutions, mercury specifically accumulated in the pronephric ducts, in the yolk sac wall (but not inside the yolk), and in the liver. Mercuric bis-L-cysteineate solutions had similar target organs, but overall levels were significantly higher, especially in the yolk sac wall.

Following exposure to organic mercury solutions, mercury specifically accumulated in the pronephric ducts, the liver, the yolk sac wall, and the somitic muscles (Figure 5). Mercury levels in the pronephric ducts and the liver were similar for both methylmercury chloride solution and methylmercury L-cysteineate exposures, reaching 0.25 and 0.19 μg/cm², respectively. Despite the higher mercury exposure concentrations used for methylmercury L-cysteineate compared with methylmercury chloride, the latter resulted in higher mercury levels in the yolk, the gut, and the medulla oblongata.

In summary, inorganic mercury exposures resulted in overall lower mercury burdens than organic mercury exposures. The difference was especially pronounced for mercuric bis-L-

cysteineate, which despite the highest concentration (200 μM) of all four forms, showed mercury levels lower than those of the organic mercury larvae, except for the yolk sac wall (Figure 5). Exposures to inorganic mercury species not only gave generally lower mercury levels but also targeted different cell types in the developing larvae. In mercuric chloride solution, the highest mercury levels were in the olfactory epithelial cells (0.05−0.16 μg/cm²) (Figure 2). For mercuric bis-L-cysteineate, the target cells were those of the yolk sac wall (0.05−0.15 μg/cm²) (Figure 5). However, by far the highest mercury levels were detected in the eye lens epithelial cells in the larvae exposed to solutions of methylmercury chloride and methylmercury L-cysteineate (0.4−0.82 and 0.4−0.96 μg/cm²) (Figure 3).

Higher bioaccumulation levels of organic mercury toxicants have been observed previously and sometimes attributed to their enhanced lipid solubility and thus higher permeability across the cell membrane. If passive diffusion of a molecule was the sole uptake mechanism, then differences in cell membrane permeabilities might alone explain the observed differential uptake of inorganic and organic mercury species herein. To test this, we estimated the permeabilities P of dominant mercury species (>1% in Table 1) as[27]

$$P = K_{ow}D_m/\lambda \tag{1}$$

where K_{ow} is the octanol−water partition coefficient, D_m is the diffusion coefficient across the cell membrane, and λ is the cell membrane thickness. D_m was estimated using the expression of Stein and Lieb,[27] relating D_m to molecular volume V and two constants, D_0 and m_V, dependent upon the nature of the biological membrane.[27]

$$\log D_m = \log D_0 - m_V V \tag{2}$$

Reliable effective molecular volumes V can be computed from three-dimensional structures,[28] and all such calculations herein were done using Accelrys Discovery Studio v3.0.0. We assumed that D_0 and m_V for zebrafish larvae approximate those for human erythrocytes, for which required data have already been reported. D_m values were calculated for 10 different non-electrolyte species using eq 1 with published values of P and K_{ow} and assuming $\lambda = 40$ Å.[27] D_0 and m_V were then computed by linear regression of a plot of logD_m against V giving $D_0 = 3.6 \times 10^{-8}$ cm²/s and $m_V = 0.0413$ Å⁻³. These values of D_0 and m_V together with computed molecular volumes V of the various mercury species were then used in eq 2 to estimate diffusion coefficients for the these species (Table 2). Permeabilities P were then estimated using eq 1 and previously published K_{ow} values (Table 2).

The calculation of D_m and P parameters for the mercury species, though applicable specifically for the red blood cell

membrane, provided an important insight into the molecular basis of the differential mercury uptake observed in this study. Mercuric bis-L-cysteineate, though more hydrophobic (higher K_{ow}) than most of the considered mercury species, had significantly decreased permeability due to its high molecular volume (Table 2). Its permeability was more than 10^4 times lower than that of the dominant hydroxide species (Table 2) thus offering a plausible explanation of its extremely low accumulation in zebrafish larvae. Despite the highest hydrophobicity among all studied forms (K_{ow} = 50), the passive diffusion of methylmercury L-cysteineate was also hindered by its much lower diffusion rate resulting in permeability similar to that of methylmercury hydroxide (Table 2).

On the basis of the permeability data alone, one would expect that, in absence of L-cysteine in the treatment solutions, the net rate of movement of inorganic mercury [90% $Hg(OH)_2$/9.5% $HgOHCl$] across the larval body (e.g., through the gills, the skin, or the gastrointestinal tract) would be similar or even slightly greater (due to a higher fraction of more permeable HgClOH species in the solution) than for organic mercury [96% CH_3HgOH/3.3% CH_3HgCl] (Table 2). This in turn would result in similar (or even slightly higher) accumulation of inorganic mercury especially in the tissues directly in contact with the surrounding water (e.g., gut epithelium). However, in contrast to methylmercury-exposed larvae, no significant accumulation of inorganic mercury occurred in the gut of the inorganic mercury-exposed fish, and thus most likely a simple passive diffusion model of a compound across the lipid part of the cell membrane cannot fully explain the differential accumulation of inorganic and organic mercury observed in our study.

Since both Hg^{2+} and $[CH_3Hg]^+$ show high affinities for thiol groups,[26] it is likely that upon entering the larval body in their original chemical form the hydroxide or chloride ligands are substituted by thiols. Hence, the likely form of mercury in tissues would be a thiolate-based one, predominantly L-cysteineate complexes, and as such distributed inside the fish body into the target cells. This may explain the observed consistency in the target organs between the chloride and the L-cysteine-based mercury treatment solutions. Significantly lower permeability of mercuric bis-L-cysteineate than methylmercury L-cysteineate may also provide a partial explanation for the generally lower mercury levels after mercuric mercury exposures in internal organs, such as liver, which are not in direct contact with the water (Figure 5). It is however clear that the preferential accumulation of extremely high levels of methylmercury in the lens epithelial cells (Figure 3) cannot be explained solely in terms of increased permeability of the thiol-bound methylmercury versus its mercuric mercury counterpart. An active transport mechanism, which is yet to be determined, must be present.

Several potential methylmercury L-cysteineate transporters have been detected or postulated in various organs and cells,[30] e.g., system L (Na$^+$-independent large neutral amino acid transporter) in the blood-brain and blood-placenta barrier and system B$^{0,+}$ (Na$^+$-dependent neutral and cationic amino acid transporter) and OAT1 (organic anion transporter 1), respectively, in the luminal and basolateral membrane of the renal proximal tubular cells. Since methylmercury uptake by eye tissues has only recently been revealed,[19,20] no data are available on possible mechanisms of its transport across cell membranes in this organ. However, the most likely candidate is system L, which is universally expressed in cells performing high protein synthesis such as the lens epithelium. Indeed, the presence of system L has been recently demonstrated both in mouse lens fiber cells[31] and in human retinal pigmented epithelial cells.[32]

Apart from the eye, organs for which a differential uptake of inorganic and organic mercury was most pronounced were the muscles and gut (Figure 5). Despite similar permeabilities between methylmercury and mercuric exposure species in absence of L-cysteine, mercury accumulated only in the gut and somitic muscles of the methylmercury-treated larvae. Moreover, the presence of L-cysteine did not affect that distribution, and only trace levels of mercury were detected in the gut and muscles of the mercury bis-L-cysteineate larvae (Figure 5). These results are consistent with previous observations of poorly absorbed inorganic mercury species in the gastrointestinal tract when compared with methylmercury species.[1] Mechanisms of mercury uptake by the gut epithelium are not fully understood in either fish or mammals; however, both passive diffusion and active transport have been implied.[30,33] The process of mercury uptake in the gut is additionally complicated by the presence of the mucosal microenvironment on the gut epithelial surface. It has been postulated that polyanionic ligands of mucus may interact with the inorganic mercury species in the gut lumen resulting in ligand exchange and transport modification across the mucosal membrane.[33] Low inorganic mercury levels observed in the somitic muscles could result directly from low absorption by the gut epithelium and thus low uptake into the blood compartment.

Although mercury accumulation within the brain was not unexpected, different chemical forms displayed very different accumulation patterns. Methylmercury exposures led to generally diffuse though high accumulations of mercury. In contrast, inorganic mercury exposures affected only specific areas of the brain with mercury levels significantly lower than those for methylmercury (Figures 3 and 4). This is consistent with previous studies and the ability of methylmercury to cross the blood-brain barrier on the system L transporter (LAT1) as methylmercury L-cysteineate species.

The most pronounced difference in brain mercury distributions between the organic and inorganic mercury treatments was the preferential accumulation of inorganic mercury in the brain ventricular region (Figures 3, 4, and 5). The cerebrospinal fluid-filled ventricles of the brain as well as the central canal of the spinal cord are lined with the ependymal cells, which are the most likely target cells for the observed inorganic mercury deposition. Mercury deposits in the cytoplasm of these cells were observed previously in rats exposed to mercuric chloride in drinking water.[34] The accumulation of mercury in ependymal cells suggests that these cells may act as a barrier to the transfer of inorganic mercury from cerebrospinal fluid (and thus the blood) to brain. Interestingly, it has been recently found that ependymal cells express high levels of selenoprotein P (Sel P) in human brain.[35] Sel P is an abundant plasma glycoprotein with an unusually high content of selenocysteine and cysteine residues (up to 10 and 17, respectively). Sel P has a significant function in selenium homeostasis,[36] in particular being implicated in selenium transport to brain.[37] Its expression in zebrafish has recently been reported.[38] Sel P appears to have a significant role in mercury sequestration. When mammals (rabbits or rats) are intravenously given equimolar solutions of sodium selenite and $HgCl_2$, the toxic effects of the mercury are relieved.[39] Gailer et al. used synchrotron-based X-ray absorption spectroscopy to show that the molecular basis of this antagonism is the

formation of nanoparticulate HgSe in blood plasma.[40] The formation of such nanoparticles was previously suggested by Suzuki and co-workers,[39] who estimated their approximate size as $(HgSe)_{100}$ and demonstrated that Sel P can sequester up to 35 of these nanoparticles.[39] In light of the binding properties of Sel P, the formation of similar complexes in the ependymal cells is thus plausible.

Despite significant differences in brain mercury distribution between different mercury treatments, we discovered preferential accumulation of mercury in the epiphysis (pineal gland) of both the inorganic and organic mercury-treated larvae (Figure 3). Mercury deposits in the pineal gland have been observed in miners exposed to elemental mercury.[41] The pineal gland lies outside the blood-brain barrier and therefore pinealocytes have free access to mercury in the bloodstream. The mechanism of mercury uptake by the pineal gland is not yet known. However, since pineal gland produces melatonin, a hormone affecting the modulation of wake/sleep patterns, the elevated mercury levels therein could be responsible for the sleep disturbances observed in mercury-intoxicated individuals.[42] A protective effect of melatonin against methylmercury-induced mortality[43] and mercuric chloride-induced oxidative damage[44] has been also reported.

Similarly to the pineal gland, all molecular forms of mercury led to accumulation in two types of sensory tissues. The olfactory epithelium (olfaction system) contains sensory hair cells responsible for detecting chemicals that elicit an olfactory response. The neuromasts of lateral line system (mechansensory system) comprise hair cells, organized into small bundles and distributed on the outside of the fish body, that detect pressure changes in water. The hair cells of both olfactory epithelium and neuromasts are in direct contact with contaminated water, and the presence of mercury is likely related to this fact. The levels of mercury accumulation in the olfactory epithelium reflected the estimated permeabilities of the different mercury species (Table 2), suggesting a prevalence of passive transport across the epithelial barrier. However, the same trend was not observed in the neuromasts. Despite similar permeabilities, inorganic mercury concentrations were on average half compared with their organic counterparts, suggesting involvement of an active carrier in the transport of methylmercury species across the cell membrane.

The uptake of inorganic and organic mercury species by the olfactory epithelium has been reported before in fish.[45] It has even been postulated that the olfactory pathway could be a route of entry for inorganic mercury species into the central nervous system.[46] In contrast, there are no available data on mercury uptake by the lateral line system; however, the disruptive effects of other heavy metals on neuromasts have been reported.[47] Interestingly, the hair cells of the neuromasts are physiologically and microscopically very similar to mammalian inner ear hair cells and as such have been recently used to screen for drugs that prevent or cause hearing loss.[48] It is thus likely that hearing problems reported previously in individuals intoxicated with mercury may be partially due to the accumulation of mercury in the inner ear hair cells. Further studies are clearly needed to confirm that.

In conclusion, synchrotron X-ray fluorescence imaging has revealed striking differences in the accumulation patterns of mercury in zebrafish larvae exposed to four different mercury formulations in water. Exposures to methylmercury species not only resulted in overall higher mercury burdens but also targeted different cells and tissues, revealing a significant role of speciation in cellular and molecular targeting and sequestration.

■ METHODS

Animal Care and Embryo Collection. Adult fish were kept at 28 °C in carbon-filtered tap water with a photoperiod of 14 h. Embryos were collected and staged following standard procedures. After collection, embryos and larvae were reared in 25-mL Petri dishes with culture water changed daily. This work was approved by the University of Saskatchewan's Animal Research Ethics Board and adhered to the Canadian Council on Animal Care guidelines on the care and use of fish in research, teaching, and testing.

Mercury Treatment Solutions. Methylmercury compounds are extremely toxic, and thus appropriate precautions must be taken to prevent any inhalation of or skin contact with these compounds or solutions thereof. All reagents, except when specifically mentioned, were purchased from Sigma-Aldrich as the highest quality available. A 1 mM stock solution of mercuric chloride was made from mercuric chloride crystals dissolved in triple-distilled water. A stock solution of 1 mM mercuric bis-L-cysteineate was prepared from 2 mM stock solution of mercuric chloride and 5 mM solution of L-cysteine in 100 mM HEPES buffer by mixing equal aliquots of those two (1:2.5 molar ratio) to ensure each mercury atom was bound to two cysteine molecules. Methylmercury chloride was purchased as a 1000 ppm aqueous solution from Alfa Aesar and further diluted in triple-distilled water to give a 1 mM stock solution. Methylmercury hydroxide was purchased as a 1 M aqueous solution from Strem Chemicals Inc. and diluted in triple-distilled water to give a 4 mM stock solution. A 4 mM stock solution of L-cysteine was prepared in 30 mM phosphate buffered saline (PBS; 153.3 mM NaCl, 4.8 mM $NaH_2PO_4 \cdot H_2O$ and 25 mM Na_2HPO_4). A 1 mM stock solution of methylmercury L-cysteineate was prepared by mixing suitable aliquots of methylmercury hydroxide and L-cysteine solutions to give a 20% molar excess of L-cysteine (*i.e.*, a molar ratio of 1:1.2) with addition of 30 mM PBS as needed.

Mercury solutions for treatment of zebrafish were prepared from the above solutions by dilution in fish culture water (carbon-filtered tap water). All stock and treatment solutions were freshly made prior to each exposure.

All exposures were at 28 °C for 36 h starting at 3.5 dpf. Larvae were placed in 25-mL Petri dishes containing 1 μM mercuric chloride (1:1000 dilution of stock solution in culture water), 200 μM mercuric bis-L-cysteineate (1:5), 1 μM methylmercury chloride (1:1000), 2 μM methylmercury L-cysteineate (1:500), or control dishes with no added mercury. For each mercury formulation (Table 1) three replicate treatments (3 × 25 larvae) were carried out. After exposure, larvae were rinsed several times in fresh carbon-filtered water to remove any remaining mercury.

Calculation of Mercury Speciation in Treatment Solutions. Mercury equilibrium speciation calculations were performed using MINTEQA2 (version 4.03), a U.S. EPA equilibrium speciation program for dilute aqueous systems.[21] The simulations were computed for 28 °C and pH 7.8, the conditions under which larvae were reared. The fish culture water was analyzed in the environmental analytical laboratory of the Saskatchewan Research Council for major components (bicarbonate, chloride, nitrate, sulfate, calcium, magnesium, potassium, sodium), and these were included in the calculations together with all of the external components originating from mercury stock solutions and PBS and HEPES buffers. The detailed list of concentrations for all of the constituents in the calculations is shown in Supplementary Table 1. Since HEPES is not included in the MINTEQA2 components, database literature values were incorporated to simulate its potential effects.[22]

Preparation of Sections. Larvae were fixed in 4% paraformaldehyde for 2 h at RT immediately following the exposures. The fixed larvae were dehydrated in a graded series (0%, 25%, 50%, 75%, and 100%) of ethanol in PBST buffer (30 mM PBS, 0.01% Tween 20) for 5 min each and stored in 100% ethanol at −20 °C until needed. For sectioning, the fixed and dehydrated larvae were rehydrated into PBST

by 5 min washes in the reversed ethanol gradient. Selected larvae were properly oriented and embedded in 1% agarose gel. The blocks of gel containing the fish were cut out and dehydrated in 100% ethanol by gentle shaking for 5−8 h at 4 °C. Following dehydration the blocks were infiltrated overnight on a rotating stirrer at 4 °C with JB-4 catalyzed solution A (10 mL solution A:0.125 g catalyst; Polysciences Inc., Warrington, PA, USA). The infiltration process with fresh infiltration solution continued on the following day for 5−6 h. The infiltrated samples were placed in embedding molds filled with a mixture of JB-4 solution B and fresh infiltration solution (1 mL solution B:25 mL infiltration solution) and left overnight at 4 °C to polymerize. Sections of 6 μm thickness were cut on a microtome using glass knives. Of two adjacent sections, one was mounted on a glass slide and stained with methylene blue, while the other, intended for synchrotron X-ray fluorescence imaging, was fixed on a Thermanox plastic coverslip (Gibco BRL) without any further processing.

X-ray Fluorescence Imaging (XFI). X-ray fluorescence images were collected at the Advanced Photon Source (Argonne, IL, USA) using beamline 20-ID-B (PNC/XOR) with the storage ring operating in continuous top-up mode at 102 mA and 7.0 GeV. The incident X-ray energy was set to 13.45 keV and the Hg L$\alpha_{1,2}$ fluorescence lines, as well as the intensity of the total scattered X-rays, were monitored using a silicon-drift Vortex detector (SII NanoTechnology USA Inc.). Incident and transmitted X-ray intensities were measured with nitrogen-filled ion chambers.

Experiments used a Si(111) double crystal monochromator and Rh-coated silicon mirrors for focusing and harmonic rejection. The microfocused beam of 5 μm diameter was generated by Kirkpatrick−Baez (K−B) Rh-coated focusing mirrors. Samples were mounted at 45° to the incident X-ray beam and were spatially rastered in the microbeam with a step size of 5 μm. Beam exposure was 0.6 s per step.

XFI Data Analysis. The XFI data were processed using SMAK software. Windowed fluorescence counts were normalized by the incident X-ray intensity and background-corrected by subtracting the average intensity obtained of pixels outside the tissue. Quantities of Hg per pixel were calibrated using two certified highly uniform thin film standards on 6.3-μm-thick mylar substrates (Micromatter, Vancouver, BC, Canada) containing 16.3 and 17.1 $\mu g/cm^2$ Au and TlCl, respectively. Using standards of gold and thallium, adjacent to mercury in the periodic table, was preferable to employing a mercury amalgam standard because the latter decreased in mercury content slowly over time, presumably due to loss of elemental mercury vapor. Average background intensities for windowed fluorescence from the standards were estimated from the X-ray fluorescence image of the 6.3-μm-thick Mylar film. The background-corrected Au and Tl L$\alpha_{1,2}$ fluorescence intensities were used to interpolate a Hg L$\alpha_{1,2}$ fluorescence intensity, which was applied to the background-corrected Hg distribution maps to obtain the quantities of Hg per pixel in $\mu g/cm^2$. The use of this unit is widespread in the XFI literature because it directly relates to what is being measured. These units can be simply related to mercury concentration in mM by assuming that the sections are uniformly 6 μm thick and by multiplying the aerial Hg densities (in $\mu g/cm^2$) by 8.3. Another useful unit is the number of moles of Hg per cell, which is sometimes used in *in vitro* uptake studies. Assuming that the average diameter of a cell is 10 μm and the thickness of the sections is 6 μm, the number of moles of Hg per cell can be calculated by multiplying the aerial Hg density (in $\mu g/cm^2$) by 4×10^{-15}. To verify the biological relevance of the aerial densities obtained with our method, we compared them to the previously reported number of moles of Hg taken up by a K-562 cell in the cell culture study following 48-h treatment with 35 μM HgCl$_2$.[49] On average, the number of moles of Hg per K-562 cell was 0.5×10^{-15}, which is only slightly higher than the respective number reported here for the zebrafish olfactory epithelial cells following 36-h exposure to 1 μM HgCl$_2$ (∼0.1 $\mu g/cm^2$ of Hg in Figure 2, corresponding to 0.4×10^{-15} mol Hg/cell).

Statistics on large sample numbers are precluded by the long data acquisition times and limited availability of synchrotron time. Instead, we examined the reproducibility in mercury levels of the liver and somitic muscles in three trunk sections following the same methylmercury L-cysteineate treatment. For different fish with identical treatments, the variation in anatomically similar sections was less than 20% (Supplementary Figure 1 and Supplementary Table 2).

In the results presented above, ranges in mercury levels refer to the observed variation from pixel to pixel in a particular area of a single sample.

■ ASSOCIATED CONTENT

ⓢ Supporting Information

This material is available free of charge *via* the Internet at http://pubs.acs.org.

■ AUTHOR INFORMATION

Corresponding Author

*E-mail: g.george@usask.ca; pat.krone@usask.ca.

Author Contributions

¶These authors contributed equally to this work.

■ REFERENCES

(1) Clarkson, T. W., and Magos, L. (2006) The toxicology of mercury and its chemical compounds. *Crit. Rev. Toxicol.* 36, 609−662.

(2) Huang, C.-F., Liu, S.-H., and Lin-Shiau, S.-Y. (2007) Neurotoxicological effects of cinnabar (a Chinese mineral medicine, HgS) in mice. *Toxicol. Appl. Pharmacol.* 224, 192−201.

(3) Mortimer, N. J., Chave, T. A., and Johnston, G. A. (2003) Red tattoo reactions. *Clin. Exp. Dermatol.* 28, 508−510.

(4) George, G. N., Singh, S. P., Hoover, J., and Pickering, I. J. (2009) The chemical forms of mercury in aged and fresh dental amalgam surfaces. *Chem. Res. Toxicol.* 22, 1761−1764.

(5) Nierenberg, D. W., Nordgren, R. E., Chang, M. B., Siegler, R. W., Blayney, M. B., Hochberg, F., Toribara, T. Y., Cernichiari, E., and Clarkson, T. W. (1998) Delayed cerebellar disease and death after accidental exposure to dimethylmercury. *N. Engl. J. Med.* 338, 1672−1676.

(6) Poulin, J., Gibb, H. (2008) Mercury: Assessing the environmental burden of disease at national and local levels. World Health Organization, Geneva, WHO Environmental Burden of Disease Series, no. 16.

(7) The Global Atmospheric Mercury Assessment: Sources, Emissions and Transport. (2008) UNEP-Chemicals, Geneva.

(8) Summary of Supply, Trade and Demand Information on Mercury. (2006) UNEP-Chemicals, Geneva.

(9) Martena, M. J., Van Der Wielen, J. C., Rietjens, I. M., Klerx, W. N., De Groot, H. N., and Konings, E. J. (2010) Monitoring of mercury, arsenic, and lead in traditional Asian herbal preparations on the Dutch market and estimation of associated risks. *Food Addit. Contam., Part A* 27, 190−205.

(10) Harris, H. H., Pickering, I. J., and George, G. N. (2003) The chemical form of mercury in fish. *Science 301*, 1203.

(11) Bravo, A. G., Loizeau, J. L., Bouchet, S., Richard, A., Rubin, J. F., Ungureanu, V. G., Amouroux, D., and Dominik. (2010) Mercury human exposure through fish consumption in a reservoir contaminated by a chlor-alkali plant: Babeni reservoir (Romania). *J. Environ. Sci. Pollut. Res. Int. 17*, 1422−1432.

(12) Trasande, L., Cortes, J. E., Landrigan, P. J., Abercrombie, M. I., Bopp, R. F., and Cifuentes, E. (2010) Methylmercury exposure in a subsistence fishing community in Lake Chapala, Mexico: an ecological approach. *Environ. Health 9*, 1.

(13) Cheng, J., Gao, L., Zhao, W., Liu, X., Sakamoto, M., and Wang, W. (2009) Mercury levels in fisherman and their household members in Zhoushan, China: impact of public health. *Sci. Total Environ. 407*, 2625−2630.

(14) Korbas, M., O'Donoghue, J. L., Watson, G. E., Pickering, I. J., Singh, S. P., Myers, G. J., Clarkson, T. W., and George, G. N. (2010) The chemical nature of mercury in human brain following poisoning or environmental exposure. *ACS Chem. Neurosci. 1*, 810−818.

(15) IPCS (1991) Inorganic mercury, World Health Organization, Geneva, International Programme on Chemical Safety, Environmental Health Criteria 118.

(16) Laks, D. R. (2009) Assessment of chronic mercury exposure within the U.S. population, National Health and Nutrition Examination Survey, 1999−2006. *Biometals 22*, 1103−1114.

(17) Yang, L., Ho, N. Y., Alshut, R., Legradi, J., Weiss, C., Reischl, M., Mikut, R., Liebel, U., Müller, F., and Strähle, U. (2009) Zebrafish embryos as models for embryotoxic and teratological effects of chemicals. *Reprod. Toxicol. 28*, 245−253.

(18) Jeong, J. Y., Kwon, H. B., Ahn, J. C., Kang, D., Kwon, S. H., Park, J. A., and Kim, K. W. (2008) Functional and developmental analysis of the blood-brain barrier in zebrafish. *Brain Res. Bull. 75*, 619−628.

(19) Korbas, M., Blechinger, S. R., Krone, P. H., Pickering, I. J., and George, G. N. (2008) Localizing organomercury uptake and accumulation in zebrafish larvae at the tissue and cellular level. *Proc. Natl. Acad. Sci. U.S.A. 105*, 12108−12112.

(20) Korbas, M., Krone, P. H., Pickering, I. J., and George, G. N. (2010) Dynamic accumulation and redistribution of methylmercury in the lens of developing zebrafish embryos and larvae. *J. Biol. Inorg. Chem. 15*, 1137−1145.

(21) http://www.epa.gov/ceampubl/mmedia/minteq/

(22) Delnomdedieu, M., Boudou, A., Georgescauld, D., and Dufourc, E. J. (1992) Specific interactions of mercury chloride with membranes and other ligands as revealed by mercury-NMR. *Chem.-Biol. Interact. 81*, 243−269.

(23) Mason, R. P., Reinfelder, J. R., and Morel, F. M. M. (1996) Uptake, toxicity, and trophic transfer of mercury in a coastal diatom. *Environ. Sci. Technol. 30*, 1835−1845.

(24) Dyrssen, D., and Wedborg, M. (1991) The sulphur-mercury(II) system in natural waters. *Water Air Soil Pollut. 56*, 507−519.

(25) Sillen, L. G. (1964) In *Stability Constants of Metal-Ion Complexes* (Sillen, L. G., Martell, A. E., Eds.), 2nd ed., pp 64, The Royal Chemical Society, London.

(26) Webb, J. L. (1966) In *Enzyme and Metabolic Inhibitors*, 1st ed., pp 729−751, Academic Press, New York.

(27) Stein, W. D., Lieb, W. R. (1986) In *Transport and Diffusion across Cell Membranes*, 1st ed., pp 69−107, Academic Press, Orlando.

(28) http://pubchem.ncbi.nlm.nih.gov/

(29) Laporte, J.-M., Andres, S., and Mason, R. P. (2002) Effect of ligands and other metals on the uptake of mercury and methylmercury across the gills and the intestine of the blue crab (*Callinectes sapidus*). *Comp. Biochem. Phys. C 131*, 185−196.

(30) Bridges, C. C., and Zalups, R. K. (2010) Transport of inorganic mercury and methylmercury in target tissues and organs. *J. Toxicol. Environ. Health, Part B 13*, 385−410.

(31) Bassnett, S., Wilmarth, P. A., and David, L. L. (2009) The membrane proteome of the mouse lens fiber cell. *Mol. Vis. 15*, 2448−2463.

(32) Yamamoto, A., Akanuma, S., Tachikawa, M., and Hosoya, K. (2010) Involvement of LAT1 and LAT2 in the high- and low-affinity transport of L-leucine in human retinal pigment epithelial cells (ARPE-19 cells). *J. Pharm. Sci. 99*, 2475−2482.

(33) Hoyle, I., and Handy, R. D. (2005) Dose-dependent inorganic mercury absorption by isolated perfused intestine of rainbow trout, Oncorhynchus mykiss, involves both amiloride-sensitive and energy-dependent pathways. *Aquat. Toxicol. 72*, 147−159.

(34) Møller-Madsen, B., and Danscher, G. (1986) Localization of mercury in the CNS of rats: Mercuric chloride per os. *Environ. Res. 41*, 29−43.

(35) Scharpf, M., Schweizer, U., Arzberger, T., Roggendorf, W., Schomburg, L., and Köhrle, J. (2007) Neuronal and ependymal expression of selenoprotein P in the human brain. *J. Neural. Transm. 114*, 877−884.

(36) Burk, R. F., and Hill, K. E. (2005) Selenoprotein P: an extracellular protein with unique physical characteristics and a role in selenium homeostasis. *Annu. Rev. Nutr. 25*, 215−235.

(37) Hill, K. E., Zhou, J., McMahan, W. J., Motley, A. K., Atkins, J. F., Gesteland, R. F., and Burk, R. F. (2003) Deletion of selenoprotein P alters distribution of selenium in the mouse. *J. Biol. Chem. 278*, 13640−13646.

(38) Tujebajeva, R. M., Ransom, D. G., Harney, J. W., and Berry, M. J. (2000) Expression and characterization of nonmammalian selenoprotein P in the zebrafish, *Danio rerio. Genes Cells 5*, 897−903.

(39) Suzuki, K. T., Sasakura, C., and Yoneda, S. (1998) Binding sites for the (Hg-Se) complex on selenoprotein P. *Biochim. Biophys. Acta 1429*, 102−112.

(40) Gailer, J., George, G. N., Pickering, I. J., Madden, S., Prince, R. C., Yu, E. Y., Denton, M. B., Younis, H. S., and Aposhian, H. V. (2000) Structural basis of the antagonism between inorganic mercury and selenium in mammals. *Chem. Res. Toxicol. 13*, 1135−1142.

(41) Falnoga, I., Tusek-Znidaric, M., Horvat, M., and Stegnar, P. (2000) Mercury, selenium, and cadmium in human autopsy samples from Idrija residents and mercury mine workers. *Environ. Res. 84*, 211−218.

(42) Kobal, A. B., and Grum, D. K. (2010) Scopoli's work in the field of mercurialism in light of today's knowledge: Past and present perspectives. *Am. J. Ind. Med. 53*, 535−547.

(43) Kim, C. Y., Nakai, K., Kameo, S., Kurokawa, N., Liu, Z. M., and Satoh, H. G. (2000) Protective effect of melatonin on methylmercury-Induced mortality in mice. *Tohoku J. Exp. Med. 191*, 241−246.

(44) Sener, H. G., Sehirli, A. O., and Ayanoglu-Dülger, G. (2003) Melatonin protects against mercury(II)-induced oxidative tissue damage in rats. *Pharmacol. Toxicol. 93*, 290−296.

(45) de Oliveira Ribeiro, C. A., Belger, L., Pelletier, E., and Rouleau, C. (2002) Histopathological evidence of inorganic mercury and methyl mercury toxicity in the arctic charr (*Salvelinus alpinus*). *Environ. Res. 90*, 217−225.

(46) Henriksson, J., and Tjälve, H. (1998) Uptake of inorganic mercury in the olfactory bulbs *via* olfactory pathways in rats. *Environ. Res. 77*, 130−140.

(47) Froehlicher, M., Liedtke, A., Groh, K. J., Neuhauss, S. C., Segner, H., and Eggen, R. I. (2009) Zebrafish (*Danio rerio*) neuromast: Promising biological endpoint linking developmental and toxicological studies. *Aquat. Toxicol. 95*, 307−319.

(48) Ou, H. C., Santos, F., Raible, D. W., Simon, J. A., and Rubel, E. W. (2010) Drug screening for hearing loss: Using the zebrafish lateral line to screen for drugs that prevent and cause hearing loss. *Drug Discovery Today 15*, 265−271.

(49) Frisk, P., Yaqob, A., Nilsson, K., Carlsson, J, and Lindh, U. (2001) Influence of selenium on mercuric chloride cellular uptake and toxicity indicating protection. *Biol. Trace Elem. Res. 81*, 229−244.